Quantum Chaos Triggered by Precursors of a Quantum Phase Transition: The Dicke Model

Clive Emary* and Tobias Brandes
Department of Physics, UMIST, P.O. Box 88, Manchester M60 1QD, United Kingdom
(Received 11 July 2002; published 27 January 2003)

We consider the Dicke Hamiltonian, a simple quantum-optical model which exhibits a zero-temperature quantum phase transition. We present numerical results demonstrating that at this transition the system changes from being quasi-integrable to quantum chaotic. By deriving an exact solution in the thermodynamic limit we relate this phenomenon to a localization-delocalization transition in which a macroscopic superposition is generated. We also describe the classical analogs of this behavior.

DOI: 10.1103/PhysRevLett.90.044101 PACS numbers: 05.45.Mt, 42.50.Fx, 73.43.Nq

At zero temperature, systems of N interacting particles can exhibit a quantum phase transition (QPT) as a function of a coupling parameter λ in the limit that $N \rightarrow \infty$. How do the precursors of such a transition influence quantum chaotic (and nonchaotic) behavior of the same system for finite N?

One of the most direct indicators of the emergence of quantum chaos is the change in energy level-spacing statistics from Poissonian to being described by the Gaussian ensembles of random matrix theory. Although this changeover has been observed in many systems [1–4], only in a comparatively few, isolated cases has the onset of quantum chaos been correlated with the presence of a QPT. Important examples include spin glass shards, which have recently been used in modeling the onset of chaos in quantum computers [5], the Lipkin model [6], the interacting boson model [7], and the three-dimensional Anderson model [8,9], where the change in level statistics occurs at the metal-insulator (localization-delocalization) transition found in disordered electronic systems.

In this Letter we consider the Dicke Hamiltonian (DH) [10], a quantum-optical model describing the interaction of N two-level atoms with a number of bosonic modes. We demonstrate that a crossover between Poisson and Wigner-Dyson statistics in this model for finite N is intimately connected to a mean-field-type superradiance QPT.

The simplicity and generality of the Dicke Hamiltonian have afforded it appeal both for the investigation of quantum chaos and as a model for phase transitions at a critical coupling λ_c induced by the interaction with light. The level statistics for finite N have revealed the existence of quantum chaos in certain isolated regimes of the model [11,12]. On the other hand, the QPT aspect for $N \rightarrow \infty$ has been discussed in the context of superradiance [13,14] and recently for exciton condensation [15]. Here, we derive an *exact* solution for all eigenstates, eigenvalues, and critical exponents in the thermodynamic limit and show that above the critical point $\lambda = \lambda_c$ the ground-state wave function bifurcates into a macroscopic superposition for any $N < \infty$. Our numerical results indicate that a localization-delocalization transition for $N \rightarrow \infty$ underlies the crossover between Poissonian and Wigner level-spacing distributions for finite N. Furthermore, we use an exact Holstein-Primakoff transformation to derive the classical limit of the model for arbitrary N and find a transition at $\lambda = \lambda_c$ from regular to chaotic trajectories. The latter are delocalized around *two* fixed points in phase space which we conjecture constitute the classical analog of the macroscopic superposition. The emergence of this state in the Dicke model is related to a conserved parity which becomes spontaneously broken in the thermodynamic limit.

We consider the single-mode Dicke Hamiltonian

$$H = \omega_0 J_z + \omega a^\dagger a + \frac{\lambda}{\sqrt{2j}}(a^\dagger + a)(J_+ + J_-), \qquad (1)$$

where J_z, $J_\pm$ are the usual angular momentum operators for a pseudospin of length $j = N/2$ and a, $a^\dagger$ are the bosonic operators of the field. The atomic level splitting is given by ω_0, ω is the field frequency, and λ is the atom-field coupling. Crucially, we have not made the rotating-wave approximation (RWA), as this would render the model integrable and destroy the phenomena that we describe here [12]. There is a conserved parity Π associated with the DH, which is given by $\Pi = \exp\{i\pi[a^\dagger a + J_z + j]\}$, such that $[H, \Pi] = 0$. The eigenvalues of Π are ± 1 and, unless stated, we work exclusively in the positive parity subspace.

We begin by discussing the properties of the system in the thermodynamic limit $N, j \rightarrow \infty$. In this limit the system becomes integrable for all λ, and we can derive effective Hamiltonians to describe the system exactly in each of its two phases. We employ a procedure similar to Hillery and Mlodinow's analysis of the RWA Hamiltonian [16] and introduce the Holstein-Primakoff representation of the angular momentum operators, $J_+ = b^\dagger\sqrt{2j - b^\dagger b}$, $J_- = \sqrt{2j - b^\dagger b}\, b$, $J_z = (b^\dagger b - j)$, where b and $b^\dagger$ are bosonic operators [17]. Making these substitutions allows us to write the DH as a two-mode Hamiltonian. Below the phase transition, we proceed to the thermodynamic limit by expanding the square roots and neglecting terms with powers of j in the denominator. This yields the effective Hamiltonian $H^{(1)} = \omega_0 b^\dagger b + \omega a^\dagger a + \lambda(a^\dagger + a)(b^\dagger + b) - j\omega_0$. This bilinear Hamiltonian may then be diagonalized to give $H^{(1)} = \varepsilon_-^{(1)} c_-^\dagger c_- + \varepsilon_+^{(1)} c_+^\dagger c_+ - j\omega_0$, where $\varepsilon_\pm^{(1)}$ are the excitation energies of the low-coupling phase and are given by

$$2(\varepsilon_\pm^{(1)})^2 = \omega^2 + \omega_0^2 \pm \sqrt{(\omega_0^2 - \omega^2)^2 + 16\lambda^2\omega\omega_0}. \quad (2)$$

The energy $\varepsilon_-^{(1)}$ is real only for $\lambda \leq \sqrt{\omega\omega_0}/2 = \lambda_c$, which locates the phase transition. We derive an effective Hamiltonian above λ_c by first displacing each oscillator mode in the Holstein-Primakoff DH by a quantity proportional to $\sqrt{j}$ and then neglecting terms as above. With an appropriate choice of displacements, this process also yields a bilinear Hamiltonian, which may be diagonalized to a form similar to $H^{(1)}$, but with different vacuum and excitation energies, the latter of which are given by

$$2\lambda_c^4(\varepsilon_\pm^{(2)})^2 = \omega_0^2\lambda^4 + \omega^2\lambda_c^4 \pm \sqrt{(\omega_0^2\lambda^4 - \omega^2\lambda_c^4)^2 + 4\omega^2\omega_0^2\lambda_c^8}. \quad (3)$$

The excitation energy $\varepsilon_-^{(2)}$ of this second Hamiltonian $H^{(2)}$ is real only above the phase transition. There are two independent choices of displacements, each of which yield a different effective Hamiltonian above λ_c. This is a consequence of the fact that at the QPT the Π symmetry is spontaneously broken.

In Fig. 1 we plot as a function of coupling the behavior of the excitation energies and the ground-state energy, which is itself continuous but possesses a discontinuity in its second derivative at λ_c. Below the phase transition the ground state is composed of an empty field with all the atoms unexcited and hence $\langle J_z\rangle_G/j = -1$ and $\langle a^\dagger a\rangle_G/j = 0$. Above λ_c, the field is macroscopically occupied, $\langle a^\dagger a\rangle_G/j = 2(\lambda^4 - \lambda_c^4)/(\omega\lambda)^2$, and the atoms acquire a macroscopic inversion, $\langle J_z\rangle_G/j = -\lambda_c^2/\lambda^2$. At the phase transition, the excitation energy ε_- vanishes as $|\lambda - \lambda_c|^{z\nu}$ and the characteristic length scale $l_- = 1/\sqrt{\varepsilon_-}$ diverges as $|\lambda - \lambda_c|^{-\nu}$, with exponents given by $\nu = 1/4$, $z = 2$ on resonance.

To investigate the level statistics of the system, we numerically diagonalize the Hamiltonian in the basis $\{|n\rangle \otimes |j, m\rangle\}$, where $a^\dagger a|n\rangle = n|n\rangle$, and $|j, m\rangle$ are the Dicke states, $J_z|j, m\rangle = (b^\dagger b - j)|j, m\rangle = m|j, m\rangle$. We restrict ourselves to the positive parity subspace by considering only states with $n + m + j$ even. We then unfold the resulting energy spectrum to rid it of secular variation, form the level spacings $S_n = E_{n+1} - E_n$, and then construct the nearest-neighbor distribution function $P(S)$. Finally, we normalize the results for comparison with the universal ensembles of random matrix theory. In the following, we use the term "quasi-integrable" to denote systems exhibiting Poissonian level statistics, and we reserve "integrable" for systems possessing exact solutions.

Figure 2 shows the $P(S)$ distributions obtained for the DH at various values of the coupling, and for various values of j. At low j the $P(S)$ clearly do not correspond to any of the universal ensembles. This is most keenly observed in the $j = 1/2$ case (identical to the Rabi Hamiltonian [18]), where the spectrum is of "picket-fence" character [19], characteristic of one-dimensional systems or harmonic oscillators [20]. For couplings less than the critical value, $\lambda < \lambda_c$, we see that as we increase j, the $P(S)$ approaches ever closer the Poissonian distribution, $P_P(S) = \exp(-S)$. At and above λ_c the spectrum is seen to converge onto the Wigner distribution $P_W(S) = \pi S/2 \exp(-\pi S^2/4)$, characteristic of quantum chaos. This demonstrates that the precursors of the QPT in this model lead to a crossover from quasi-integrable to quantum chaotic behavior at $\lambda \approx \lambda_c$.

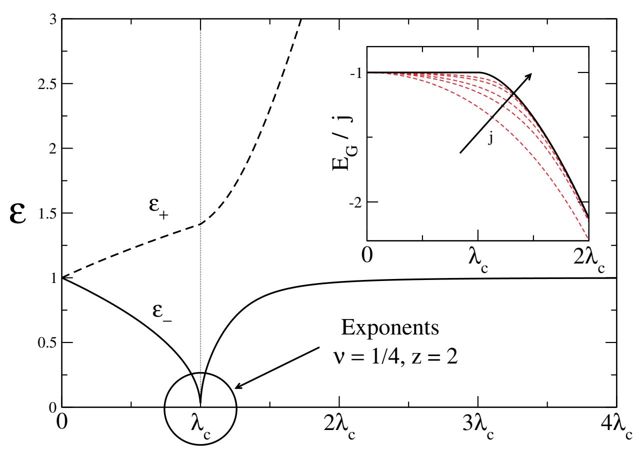

FIG. 1 (color online). Excitation energies $\varepsilon_\pm$ of the DH in the thermodynamic limit. Inset: scaled ground-state energy, E_G/j, in the thermodynamic limit (solid line) and at various finite values of $j = 1/2, 1, 3/2, 3, 5$ (dashed lines). The Hamiltonian is on scaled resonance $\omega = \omega_0 = 1$.

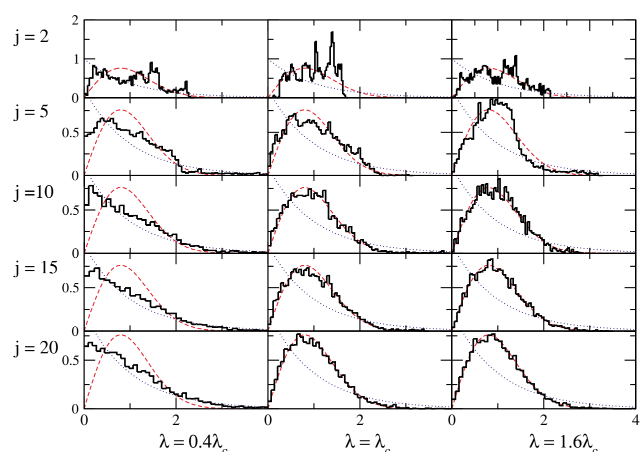

FIG. 2 (color online). Plots of nearest-neighbor distributions $P(S)$ for the Dicke Hamiltonian, for different couplings λ and pseudospin j. Also plotted are the universal Poissonian (dots) to Wigner (dashes) distributions.

A further transition between integrable and chaotic behavior is observed in the sequence of level spacings S_n. The $\lambda \rightarrow \infty$ limit of the Hamiltonian is integrable for arbitrary j, having eigenenergies $E_{nm} = \frac{\omega}{j} n - \frac{2\lambda^2}{\omega j^2} m^2$, where $n = 0, 1, 2, \ldots$ and $m = -j, \ldots, +j$. As λ is increased from λ_c to approach this limit with j fixed, the spectrum reverts from Wignerlike to integrable. However, it does not follow the usual transition sequence, but rather through a sequence illustrated by Fig. 3. The spectrum becomes very regular at low energy, where it approximates the integrable $\lambda \rightarrow \infty$ results closely. Outside the regular region the spectrum is well described by the Wigner surmise, and the energy scale over which the change between the two regimes occurs is seen to be surprisingly narrow. As coupling is increased, the size of the low-energy integrable window increases, until it eventually engulfs the whole spectrum as $\lambda \rightarrow \infty$.

We now proceed to consider the wave functions of the system by introducing an abstract position-momentum representation for each of the boson modes via $x \equiv (1/\sqrt{2\omega})(a^\dagger + a)$; $p_x \equiv i\sqrt{\omega/2}(a^\dagger - a)$, and $y \equiv (1/\sqrt{2\omega_0})(b^\dagger + b)$; $p_y \equiv i\sqrt{\omega_0/2}(b^\dagger - b)$. In this representation the action of the parity operator Π corresponds to rotation by π about the origin. The ground state of the system on scaled resonance for $j = 5$ is plotted for different couplings in Fig. 4. These wave functions were obtained by diagonalizing the Hamiltonian in the same basis as was used to calculate $P(S)$ and representing the basis vectors $|n\rangle \otimes |m, j\rangle$ by products of harmonic oscillator eigenfunctions. For the noninteracting system ($\lambda = 0$), the wave function is a product of two independent Gaussians. As the coupling increases, the two modes start mixing, leading to a stretching of the single-peaked wave function. Around the critical coupling ($\lambda \approx \lambda_c$), the wave function bifurcates to become a double-peaked function, and with further increases in coupling the two lobes at $(\pm x_0, \mp y_0)$ move away from each other in their respective quadrants of the x-y plane. Since x_0 and y_0 are of the order of $\sqrt{j}$, for large j the ground state evolves into a superposition of two macroscopically distinguishable parts, which may be considered as a "Schrödinger's cat." The formation of this state constitutes a delocalization of the ground-state wave function, which is also observed in the excited states. This localization-delocalization transition is consistent with the transition between Poisson and Wigner distributions in the spectrum [21]. The suppression of chaos at low j is then seen to be due to the fact that for low j only a few excitations are permitted in the b mode. This restricts the extent of the wave function in the y direction, inhibiting delocalization, and yielding the nongeneric $P(S)$ seen in Fig. 2. It should be noted that an actual spontaneous symmetry-breaking transition occurs above λ_c in the $j \rightarrow \infty$ limit which removes the two lobes so far from one another that they cease to overlap and thus can be considered independently. This breaks the Π symmetry of the model, allowing us to obtain the earlier exact results by using an effective Hamiltonian for each lobe. These Hamiltonians are identical in form, have identical spectra, thus demonstrating that in the thermodynamic limit, each energy level in the high-coupling phase is doubly degenerate and the macroscopic superposition is broken in half.

Finally, this position representation allows us to study the classical analogs of this QPT and the accompanying onset of chaos in a very natural way. By setting the commutators $[x, p_x]$ and $[y, p_y]$ to zero, the classical Hamiltonian corresponding to Eq. (1) is seen to be

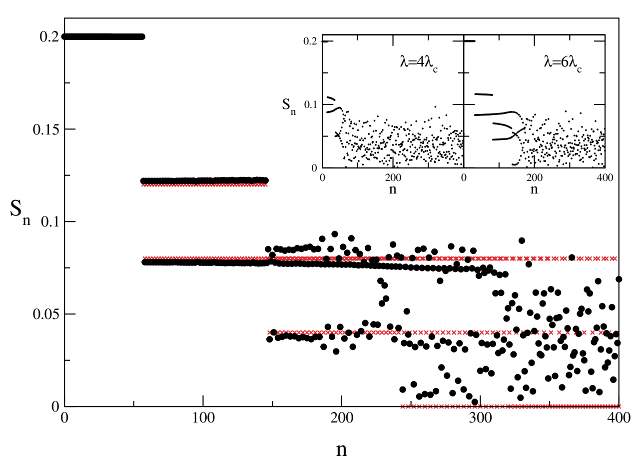

FIG. 3 (color online). Nearest-neighbor spacing $S_n = E_{n+1} - E_n$ vs eigenvalue number n plot for $j = 5$ with $\lambda = 8\lambda_c$. Horizontal crosses: results for the integrable $\lambda \rightarrow \infty$ Hamiltonian. Inset: $j = 5$ results with $\lambda = 4\lambda_c$ and $\lambda = 6\lambda_c$.

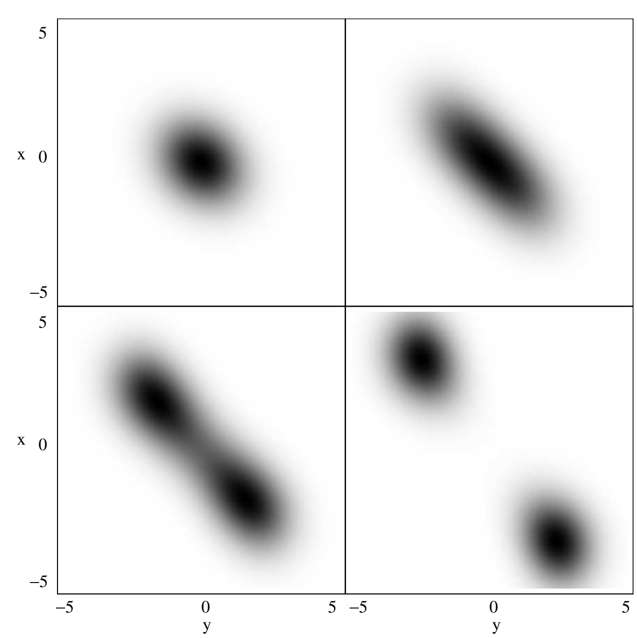

FIG. 4. The modulus of the ground-state wave function $\psi(x, y)$ of the Dicke Hamiltonian in the abstract x-y representation for finite $j = 5$, at couplings of $\lambda/\lambda_c = 0.4, 1.0, 1.2, 1.4$. Black corresponds to $\max|\psi|$ and white corresponds to zero.

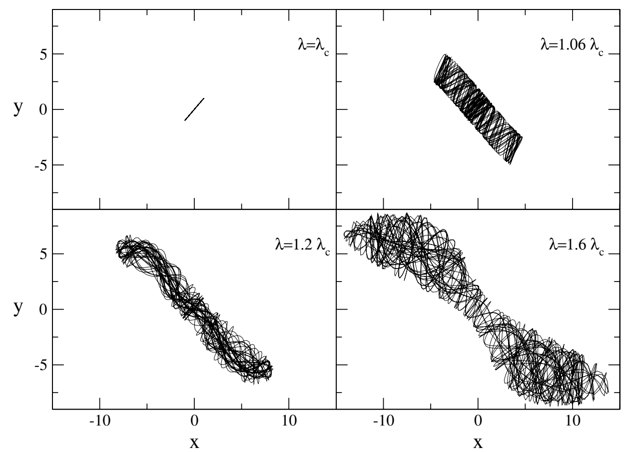

FIG. 5. Typical classical phase space projections ($p_x = p_y = 0$) for the classical Dicke Hamiltonian of Eq. (4) with $\lambda/\lambda_c = 1.0, 1.06, 1.2, 1.6$, for $j = 30.0$, $\omega = \omega_0 = 1$. Initial conditions were $x(0) = y(0) = 1$, $p_x(0) = p_y(0) = 0$. The abrupt change to complex motion is observed above $\lambda = \lambda_c$.

$$H_{\rm cl} = -j\omega_0 + \frac{1}{2}(\omega_0^2 y^2 + p_y^2 + \omega^2 x^2 + p_x^2 - \omega - \omega_0) + 2\lambda\sqrt{\omega\omega_0}xy\sqrt{1 - \frac{1}{4\omega_0 j}(\omega_0^2 y^2 + p_y^2 - \omega_0)}. \tag{4}$$

Space limitations here allow us to point out only two significant features. First, below λ_c there is only one fixed point of the flow, namely, $x = y = p_x = p_y = 0$. At $\lambda = \lambda_c$ this situation changes abruptly and two new fixed points appear at $(x, y) = (\pm x_{cl}, \mp y_{cl})$ with $p_x = p_y = 0$, where x_{cl} and y_{cl} are approximately equal to the centers of the wave function lobes x_0, y_0 for large j. Second, parametric plots of typical trajectories obtained from Eq. (4) (Fig. 5) demonstrate that the system undergoes a rapid change at $\lambda = \lambda_c$ from a very simple quasiperiodic motion to intricate chaotic behavior, in agreement with the results of the quantum model. Note that the correspondence between this classical system and the original quantum one is significantly greater than previous semiclassical treatments [22], and that this holds for any j, not just for $j \to \infty$.

We mention that larger system sizes are required to check if there exists a critical level statistics of our model at λ_c [9], and that an examination of the exceptional points [6] of this model may yield further insight. Future work also includes a study of related models to determine the generality of the features described here.

In summary, we have seen that the $P(S)$ distribution of the DH at finite N changes from being Poissonian to Wigner at approximately λ_c, indicating the emergence of quantum chaos. The ground-state wave function bifurcates at this point, forming a macroscopic superposition. The underlying quantum phase transition is reflected in the classical model derived here by the appearance of two new fixed points at λ_c, where a transition between regular and chaotic trajectories occurs.

This work was supported by projects EPSRC GR44690/01, DFG Br1528/4-1, the WE Heraeus Foundation, and the U.K. Quantum Circuits Network.

*Electronic address: emary@theory.phy.umist.ac.uk

[1] T. Guhr, A. Müller-Groeling, and H. A. Weidenmüller, Phys. Rep. **299**, 189 (1998); F. Haake, *Quantum Signatures of Chaos* (Springer, Berlin, 2001).
[2] O. Bohigas, M. J. Giannoni, and C. Schmidt, Phys. Rev. Lett. **52**, 1 (1984).
[3] D. Delande and J. C. Gay, Phys. Rev. Lett. **57**, 2006 (1986).
[4] Ph. Jacquod and D. L. Shepelyansky, Phys. Rev. Lett. **79**, 1837 (1997).
[5] B. Georgeot and D. L. Shepelyansky, Phys. Rev. Lett. **81**, 5129 (1998); Phys. Rev. E **62**, 3504 (2000).
[6] W. D. Heiss and A. L. Sannino, Phys. Rev. A **43**, 4159 (1991); W. D. Heiss and M. Müller, Phys. Rev. E **66**, 016217 (2002).
[7] Y. Alhassid and N. Whelan, Nucl. Phys. **A556**, 42 (1993); P. Cejnar and J. Jolie, Phys. Rev. E **58**, 387 (1998).
[8] For a review, see P. A. Lee and T. V. Ramakrishnan, Rev. Mod. Phys. **57**, 287 (1985).
[9] I. K. Zharekeshev and B. Kramer, Phys. Rev. B **51**, 17 239 (1995); Phys. Rev. Lett. **79**, 717 (1997).
[10] R. H. Dicke, Phys. Rev. **93**, 99 (1954).
[11] R. Graham and M. Höhnerbach, Phys. Rev. Lett. **57**, 1378 (1986).
[12] C. H. Lewenkopf, M. C. Nemes, V. Marvulle, M. P. Pato, and W. F. Wrenszinski, Phys. Lett. A **155**, 113 (1991).
[13] K. Hepp and E. H. Lieb, Ann. Phys. (N.Y.) **76**, 360 (1973); Y. K. Wang and F. T. Hioe, Phys. Rev. A **7**, 831 (1973).
[14] A. V. Andreev, V. J. Emel'yanov, and Yu. A. Il'inskii, *Cooperative Effects in Optics* (IOP Publishing, Bristol, 1993); M. G. Benedict *et al.*, *Super-Radiance* (IOP Publishing, Bristol, 1996).
[15] P. R. Eastham and P. B. Littlewood, Phys. Rev. B **64**, 235101 (2001).
[16] M. Hillery and L. D. Mlodinow, Phys. Rev. A **31**, 797 (1985).
[17] T. Holstein and H. Primakoff, Phys. Rev. **58**, 1098 (1949).
[18] I. I. Rabi, Phys. Rev. **51**, 652 (1937); R. F. Bishop and C. Emary, J. Phys. A **34**, 5635 (2001).
[19] M. Kus, Phys. Rev. Lett. **54**, 1343 (1985).
[20] M. V. Berry and M. Tabor, Proc. R. Soc. London A **356**, 375 (1977).
[21] S. Fishman, D. R. Grempel, and R. E. Prange, Phys. Rev. Lett. **49**, 509 (1982); Phys. Rev. A **29**, 1639 (1984); R. E. Prange, in *Quantum Chaos*, edited by H. A. Cerdeira, R. Ramaswamy, M. C. Gutzwiller, and G. Casati (World Scientific, Singapore, 1991).
[22] P. W. Milonni, J. R. Ackerhalt, and H. W. Galbraith, Phys. Rev. Lett. **50**, 966 (1983); R. Graham and M. Höhnerbach, Z. Phys. B **57**, 233 (1984).